The Effect of Vehicle Tie Angle on the Car Deck Lashing System Safety Factor of a Ro-Ro Ferry

Alamsyah
Department of Naval Architecture, Institut Teknologi Kalimantan, Balikpapan, Indonesia | Center of Maritime Infrastructure Engineering, Institut Teknologi Kalimantan, Balikpapan, Indonesia
alamsyah@lecturer.itk.ac.id (corresponding author)

Suardi
Department of Naval Architecture, Institut Teknologi Kalimantan, Balikpapan, Indonesia
suardi@lecturer.itk.ac.id

Wira Setiawan
Department of Naval Architecture, Institut Teknologi Kalimantan, Balikpapan, Indonesia
wira@lecturer.itk.ac.id

M. Uswah Pawara
Department of Naval Architecture, Institut Teknologi Kalimantan, Balikpapan, Indonesia
uswah.pawara@lecturer.itk.ac.id

Hariyono
Department of Naval Architecture, Institut Teknologi Kalimantan, Balikpapan, Indonesia
hariyono@lecturer.itk.ac.id

Chris Jeremy Verian Sitorus
Department of Naval Architecture, Institut Teknologi Kalimantan, Balikpapan, Indonesia
chris.sitorus@lecturer.itk.ac.id

Ardi Firmansyah
Department of Naval Architecture, Institut Teknologi Kalimantan, Balikpapan, Indonesia
09221031@student.itk.ac.id

Muhammad Malik Fahad Abdulloh
Department of Naval Architecture, Institut Teknologi Kalimantan, Balikpapan, Indonesia
09211038@student.itk.ac.id

Daeng Paroka
Department of Ocean Engineering, Engineering Faculty, Hasanuddin University, Gowa, Indonesia
dparoka@eng.unhas.ac.id

Andi Ardianti
Department of Naval Architecture, Engineering Faculty, Hasanuddin University, Gowa, Indonesia
a.ardianti@unhas.ac.id

Received: 26 December 2025 | Revised: 9 February 2026 and 19 February 2026 | Accepted: 22 February 2026

 DOI: https://doi.org/10.48084/etasr.17178

ABSTRACT

This study investigates the vehicle lashing system implemented short crossing routes, such as the Balikpapan-Penajam Paser Utara route. Regulations stipulate that the maximum engagement angle should be 60°; however, they do not specify an explicit safety factor for the lashing system. Thus, this study focuses on the influence of vehicle tie angle on the safety factor of the lashing system. Modeling of the existing mild steel lashing system was carried out using Finite Element Method (FEM) numerical simulations to calculate the safety factor of the vehicle lashing system against the engagement angle, as specified in Indonesian government regulations. The results show that for all lashing system models, the von Mises stress increases linearly with the magnitude of the applied engagement angle. For Model 1, the safety factor was less than 1.0, indicating that the model is unsafe at lashing angles of 70° and 90. In contrast, other models were safe at higher lashing angles, especially Model 4, which exhibited the highest safety factor at lashing angles ranging from 30 to 90°. These results provide input to the government to consider increasing the upper limit of the vehicle system lashing angle in the regulation. A higher lashing angle will create more space on the deck of the Roll-On-/Roll-Off (Ro-Ro) ferries, potentially increasing the income of ferry operators.

Keywords-lashing system; Ro-Ro ferry; tie angle; FEM; safety factor

I. INTRODUCTION

Shipwrecks and fires have increased significantly since 2021 [1, 2]. According to the KNKT, passenger ships often experience accidents, with ferry accidents happening each year in the last five years [3]. With a high width-to-draft ratio, domestically built ferries have stability arms that achieve a heel angle of less than 25°, which does not meet IMO criteria [4, 5]. The handling of cargo on Ro-Ro ferries varies depending on on-board load distribution, which impacts the stability, strength, and safety of the vessel.

The Indonesian government has established regulations for vehicle tie-down systems on ships [6-8]. However, when used in the field, they are less effective at short distances. Tied-down vehicles can also shift or roll over due to poor tie-down systems or tie-down strength that cannot withstand forces and moments. The geometry and center of gravity of an object relative to a baseline determine its transverse motion [9, 10]. Differences in weight distribution on the vehicle deck have been the basis for previous research on ferry safety. Experiments have been conducted without considering the possibility of the vehicle sliding or rolling over [11, 12]. Previous studies on the possibility of vehicle shifting or overturning reviewed lateral accelerations caused by the ship's motion based on its position on the ship [13] and tested lateral acceleration prediction models based on the IMO second-generation stability standards [14]. Authors in [15, 16] examined the vertical and lateral accelerations of vehicles based on their positions [15]. Lateral and vertical forces were used as a reference for conducting an initial safety assessment of the Ro-Ro ferry. This study focuses on the effect of the vehicle's lashing angle on the safety factor value.

II. METHODOLOGY

A. Ship Motion

A ship always experiences three translational motions—surging, swaying, and heaving—and three rotational motions—rolling, pitching, and yawing—finding the Response Amplitude Operator (RAO) when subjected to waves from the side [17-21]. The wave height affects the vertical and lateral acceleration of each ship, as well as the ship's position [16, 22]. A typical ship motion dynamic is shown in Figure 1.

B. Lateral and Vertical Acceleration

Lateral acceleration is the change in velocity in the lateral or horizontal direction due to turns or lateral movement. It is measured in m/s², and is usually expressed as the centrifugal acceleration experienced by passengers or objects in the vehicle. Similarly, vertical acceleration refers to the change in velocity of an object in the vertical or perpendicular direction to the Earth's surface. Ocean waves, shocks, or heaving motion are some factors that can cause vertical acceleration [15, 16]. Figure 2 depicts a vehicle subjected to the lateral and vertical accelerations. The motion begins with the beam sea striking the side of the ship. This creates a rotational or rolling motion on the ferry, producing lateral and vertical accelerations on each vehicle on the ferry deck. The resultant of these two accelerations is used to calculate the forces applied to the vehicle's lashing system.

C. Angle of the Lashing System

Indonesian government regulations specify an engagement angle between 20 and 60°, relative to the deck plane [6-8]. To test these regulations, the presented study simulated a truck with engagement angles of 70° and 90°. The influence of the engagement angle on vehicle space availability is linear; however, safety factors require further investigation. Figure 3 displays different types of vehicle tie-down angles to the ferry deck. The larger the tie-down angle, the more space the vehicle has available, and vice versa.

D. The von Misses Stress

Normal, shear, and von Mises stresses are commonly used in structural analysis [23-25]. Among these, the von Mises stress is the most important parameter in numerical simulation as it represents stress in all directions [26, 27].

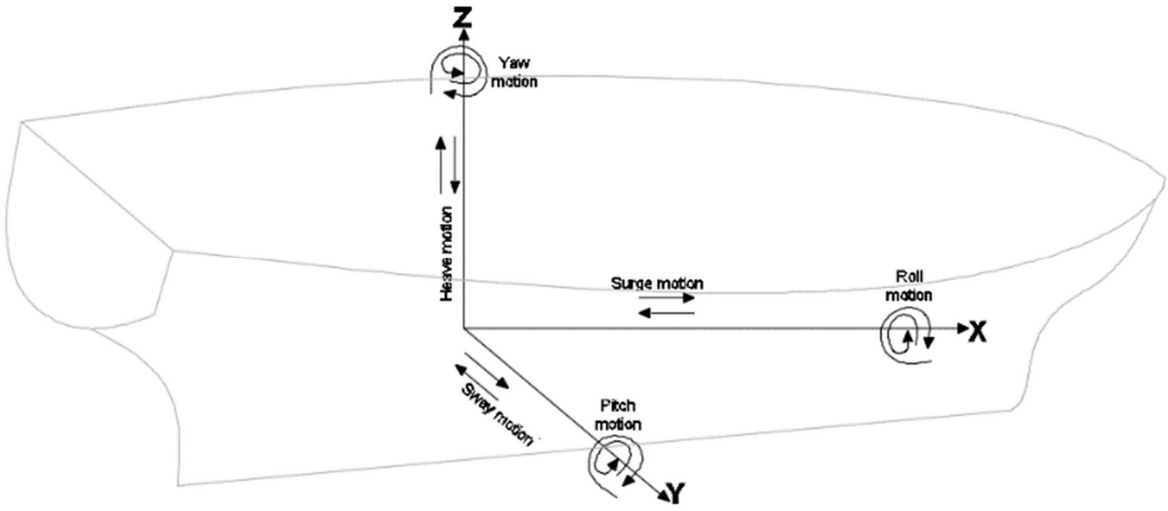

Fig. 1. Typical ship motion dynamics [22].

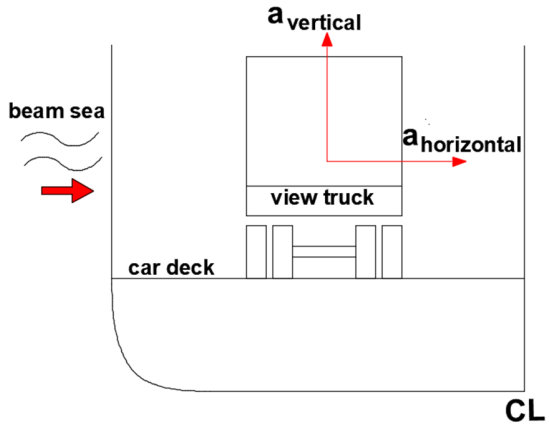

Fig. 2. Free Body Diagram of lateral and vertical acceleration on feries.

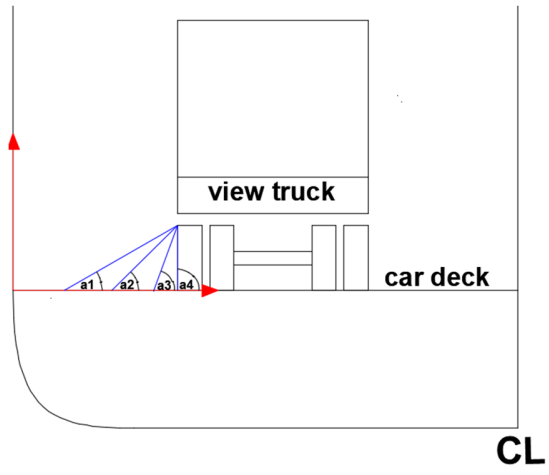

Fig. 3. Freebody diagram of vehicle tie angle.

The von Mises stress is given by [28]:

$$\sigma_v = \sqrt{\frac{1}{2}\begin{bmatrix}(\sigma_x-\sigma_y)^2+(\sigma_y-\sigma_z)^2\\+(\sigma_z-\sigma_x)^2\\+6(\tau_{xy}^2+\tau_{yz}^2+\tau_{zx}^2)\end{bmatrix}} \quad (1)$$

where σ_v is the von Mises stress, σ_x, σ_y, and σ_z are normal stresses, and τ_{xy}, τ_{yz}, and τ_{zx} are the shear stresses.

E. Safety Factor

The safety factor, as defined in (2), is the ratio of the yield stress of the material to the von Mises stress [28]. For steel, the yield strength ranges from 235 to 250 MPa, the tensile strength ranges from 400 to 510 MPa, the elongation ranges from 20 to 30%, and the modulus of elasticity ranges from 200 to 210 GPa. The safety factor is given by:

$$S_f = \frac{\sigma_{yield}}{\sigma_v} \quad (2)$$

F. Finite Element Method

FEM is a numerical method used for the analysis of the elastic-plastic behavior of materials. Several factors influence the behavior of materials, including geometry, material properties, load characteristics, initial material imperfections, boundary conditions, and local damage due to corrosion, cracks, and stress concentrations. FEM is often employed for safety analysis of ships as well as other significant components of a ship [29-33].

III. RESULTS

The Balikpapan-Penajam Paser Utara route was selected as the case study. Table I provides details of the Ro-Ro ferry used for simulation. Based on observation at the Balikpapan-Penajam Paser Utara crossing route and [22], a truck located on the centerline was selected as the sample vehicle. The resultant force (F_R) acting on the vehicle due to beam sea at the sailing wave height can be calculated using:

$$\sum F = ma \quad (3)$$

where F is the force (N), m is the mass (kg), and a is the acceleration due to gravity (m/s^2).

$$F_R = \sqrt{F_L^2 + F_V^2} \quad (4)$$

$$F_L = ma_L \quad (5)$$

where F_L is the lateral force (N), F_R is the resultant force, and a_L is the lateral acceleration (m/s^2).

$$F_V = ma_V \quad (6)$$

where F_V is the vertical force (N), and a_V is vertical acceleration (m/s^2). The resultant force is produced by the roll motion and wave direction from the side (90°).

The ferry parameters include center of gravity ($H_{vertical}$ = 1.12 m), moment of inertia (I = 538 kg.m²), resultant force (F_R = 6925 N), and roll moment (M = 3138 Nm). Moreover, the truck has the highest probability of shifting and rolling at an angle of 30.96°. These parameters represent the maximum values for a ferry car often used on the selected route. Furthermore, simulations were carried out for various lashing angles, including 30°, 45°, 70°, and 90°. The magnitude of the lashing angle has a significant impact on the resultant force acting on the ship. Table I presents the details of the Ro-Ro ferry.

TABLE I. DETAILS OF RO-RO FERRY

Parameter	Value
Length overall (LOA)	56.09 m
Length of perpendicular (LPP)	40.00 m
Breadth (B)	14.00 m
Height (H)	3.00 m
Draft (T)	2.00 m
Gross tonnage (GT)	547

TABLE II. RESULTANT FORCE FOR DIFFERENT LASHING ANGLES

Lashing angle	30°	45°	70°	90°
Resultant force on truck (N)	3463	4897	6507	6925

The study focuses on lashing angles of 70° and 90°, which they are higher than the maximum specified values for lashing angles. Similar research has been conducted to find new methods for lashing ship cargo at different lashing angles [34, 35]. The lashing system simulated in the present study is in accordance with existing field survey data and standards. Figure 4 illustrates the existing lashing system on the Balikpapan-Penajam Paser Utara ferry route.

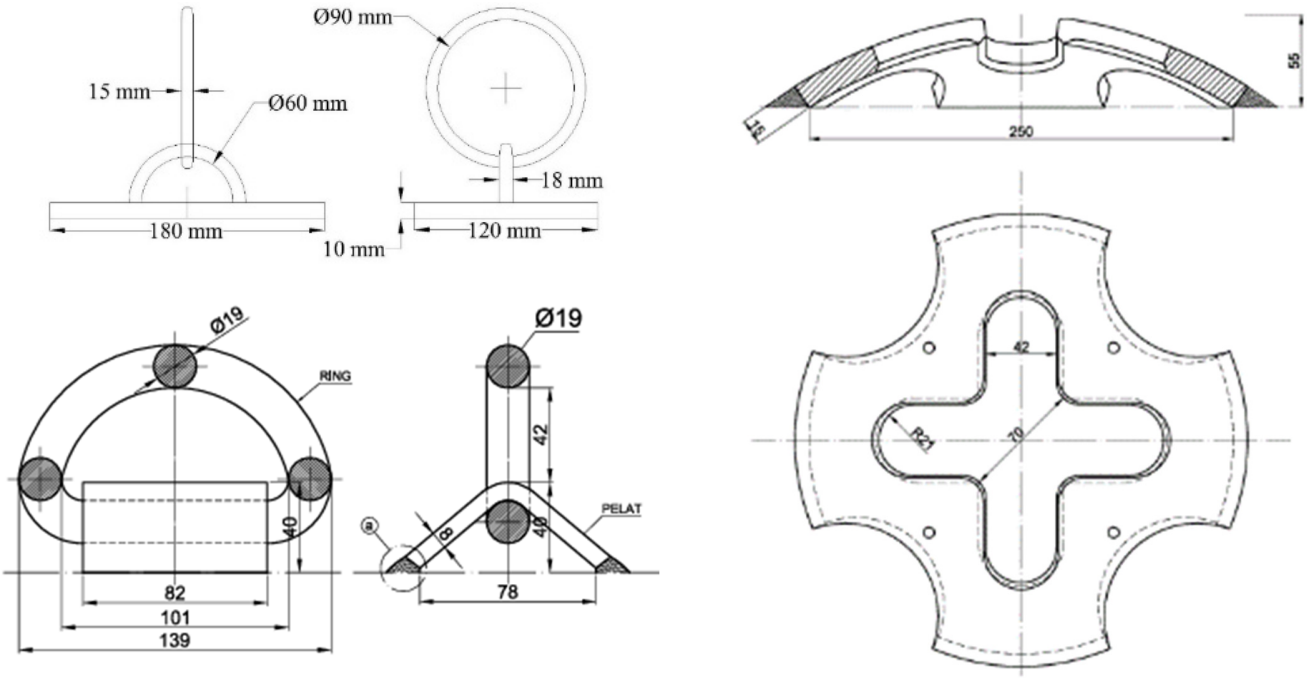

Fig. 4. Existing lashing system on the Balikpapan-Penajam Paser Utara ferry route.

Numerical simulation using FEM [36-38] was employed to analyze the existing model (Model 1) and the proposed models (Models 2-5). The latter were subjected to environmental factors, represented by reduced dimensions due to corrosion. Mesh control was applied using tetrahedral and hexahedral elements. The meshing details are presented in Table III, while Figure 5 portrays the results of the mesh convergence study. Mesh convergence analysis was conducted using the smart mesh technique, which resulted in an effective mesh size of 2 mm, as shown in Figure 5.

Figures 7-11 show the results of the model analysis using FEM. Each model was first created in 3D, followed by the assignment of boundary conditions in the form of loads according to the lashing system angles presented in Table II. The analysis yields results in the form of von Mises stress for each corresponding lashing angle. These stress values were

then utilized to calculate the safety factor using (2). The von Mises stress and safety factor for different lashing angles are depicted in Tables IV and V, respectively.

TABLE III. MESH DETAILS

Mesh size (mm)	Number of nodes	Number of elements	Force (N)	Stress (MPa)
1.6	460,144	107,735	3,463	121.40
1.8	317,408	73,355	3,463	121.45
2.0	268,359	69,863	3,463	121.50
2.2	175,536	39,732	3,463	89.50
2.4	147,324	33,206	3,463	81.56

As shown in Table V, the safety factor values for Model 1 were 0.78 and 0.74 for lashing angles of 70° and 90°, respectively, revealing that the Model was unsafe, as safety factors were less than 1.0. These results indicate that lashing angles between 70° and 90° could lead to an accident and should not be used. In contrast, Model 4 had the highest safety factors, ranging from 92.02 to 46.02, indicating that this model is significantly safer compared to other models. This applies to both small and large lashing angles, 70° and 90°.

TABLE IV. FEM SIMULATION RESULTS FOR DIFFERENT LASHING ANGLES

Lashing System	von Mises stress (MPa)			
	30°	45°	70°	90°
Model 1	169.56	239.77	318.61	339.07
Model 2	64.75	91.57	121.68	129.50
Model 3	107.68	152.27	202.33	215.33
Model 4	2.71	3.84	5.10	5.43
Model 5	3.02	4.27	5.67	6.04

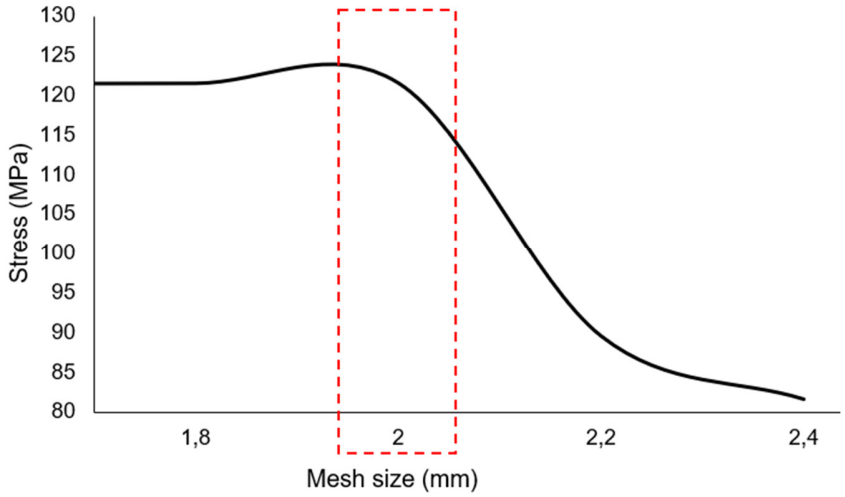

Fig. 5. Results of the mesh convergence study.

(a)

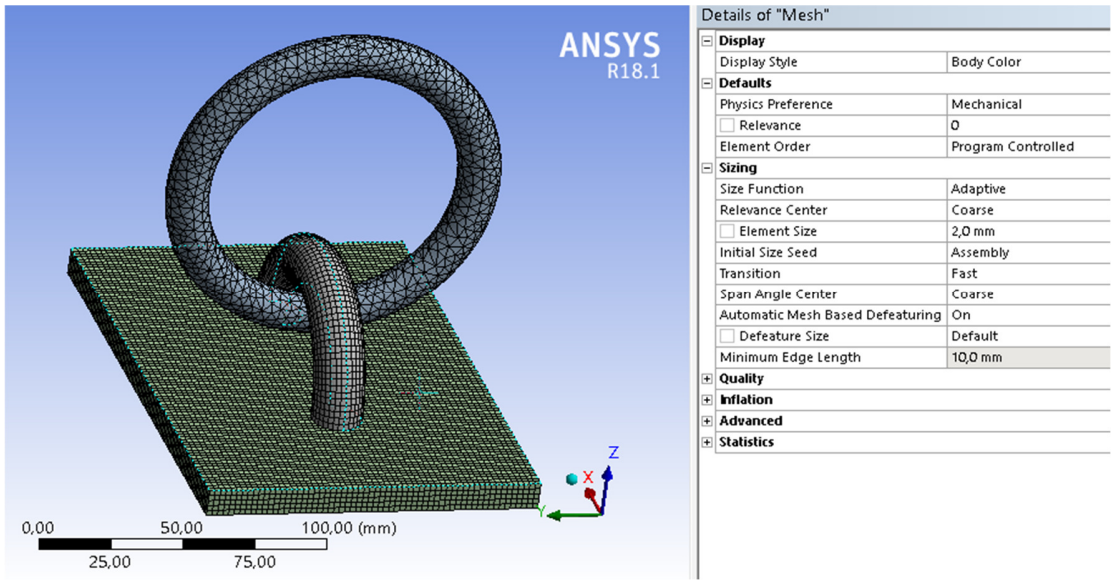

(b)

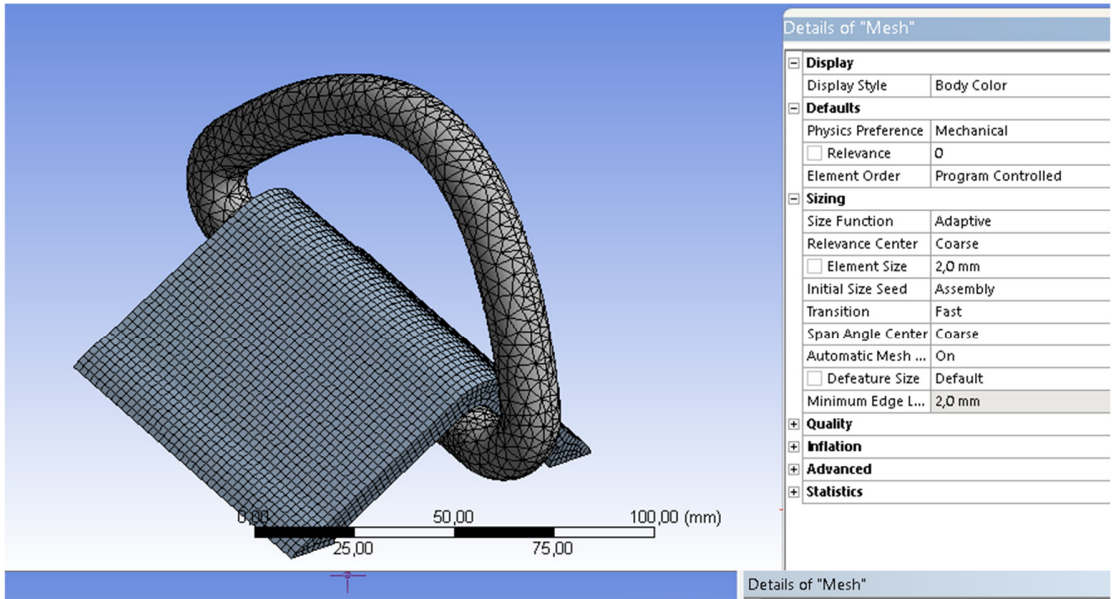
Details of "Mesh"
Display
Display Style | Body Color
Defaults
Physics Preference | Mechanical
Relevance | 0
Element Order | Program Controlled
Sizing
Size Function | Adaptive
Relevance Center | Coarse
Element Size | 2,0 mm
Initial Size Seed | Assembly
Transition | Fast
Span Angle Center | Coarse
Automatic Mesh ... | On
Defeature Size | Default
Minimum Edge L... | 2,0 mm
Quality
Inflation
Advanced
Statistics
0,00
50,00
100,00 (mm)
25,00
75,00

(c)

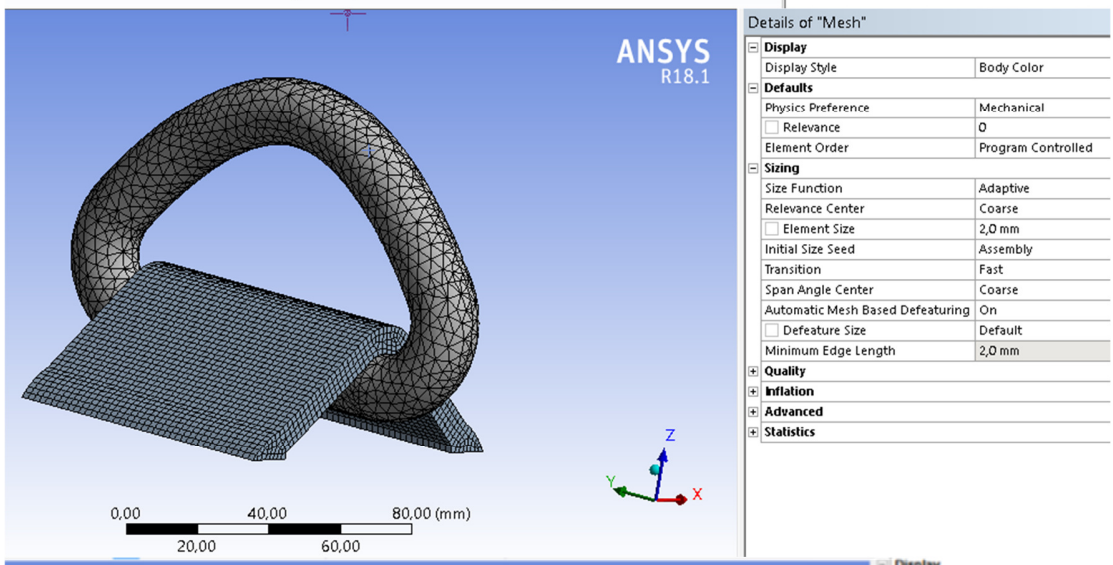
ANSYS
R18.1
Details of "Mesh"
Display
Display Style | Body Color
Defaults
Physics Preference | Mechanical
Relevance | 0
Element Order | Program Controlled
Sizing
Size Function | Adaptive
Relevance Center | Coarse
Element Size | 2,0 mm
Initial Size Seed | Assembly
Transition | Fast
Span Angle Center | Coarse
Automatic Mesh Based Defeaturing | On
Defeature Size | Default
Minimum Edge Length | 2,0 mm
Quality
Inflation
Advanced
Statistics
0,00
40,00
80,00 (mm)
20,00
60,00
Z
Y
X

(d)

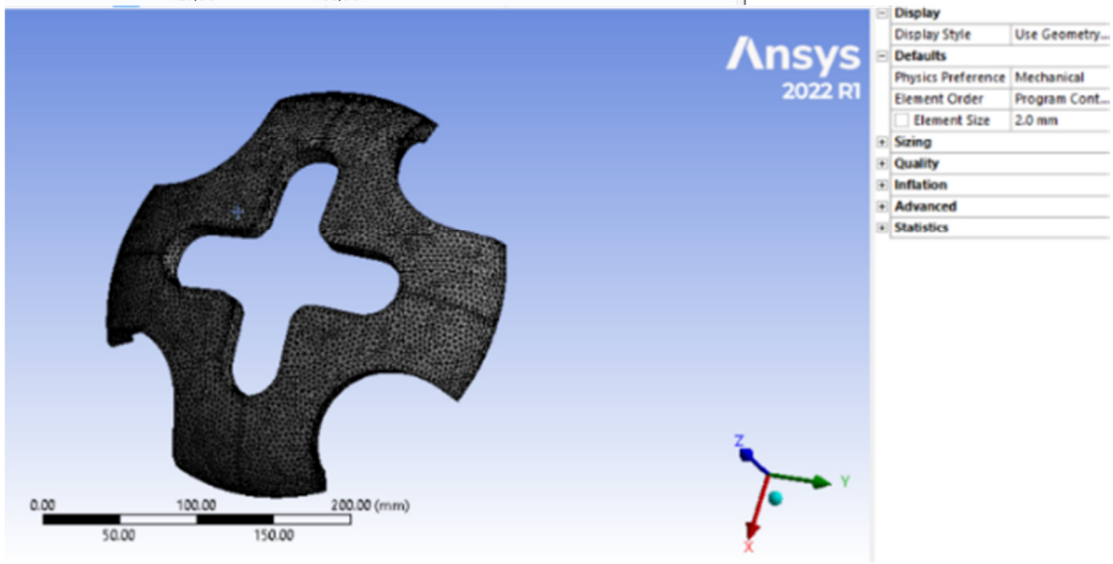
Ansys
2022 R1
Display
Display Style | Use Geometry...
Defaults
Physics Preference | Mechanical
Element Order | Program Cont...
Element Size | 2.0 mm
Sizing
Quality
Inflation
Advanced
Statistics
0.00
100.00
200.00 (mm)
50.00
150.00
Z
Y
X

(e)

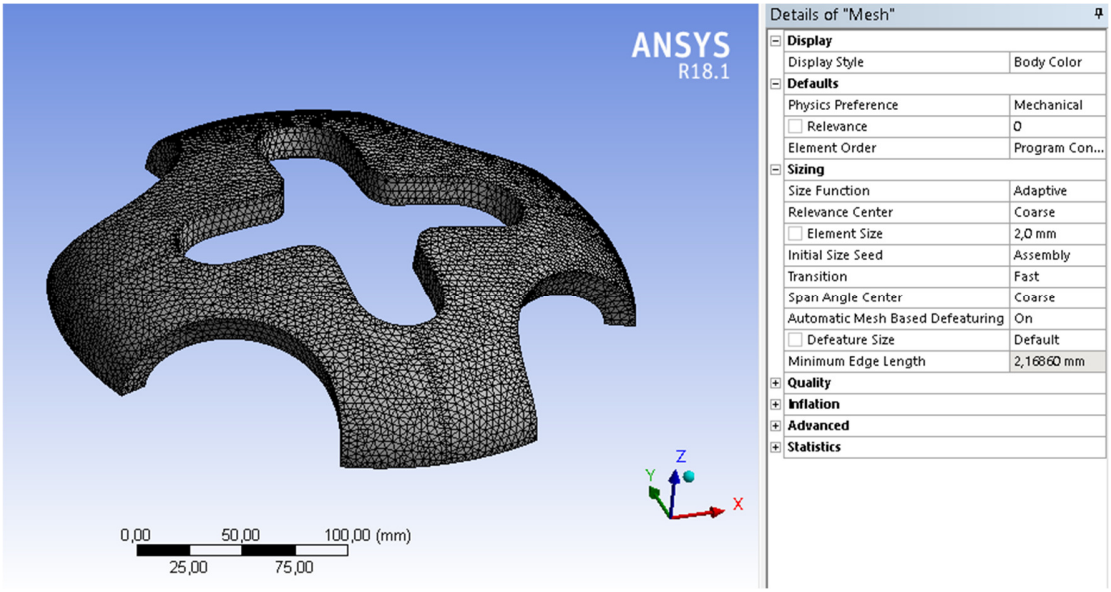

Fig. 6. Modeling of lashing system for Ro-Ro ferry: (a) Model 1, (b) Model 2 with D-ring, (c) Model 3 with D-ring subjected to 20% diameters reduction, (d) Model 4 with convex, and (e) Model 5 with convex subjected to external radius reduction.

TABLE V. CALCULATED SAFETY FACTOR FOR DIFFERENT LASHING ANGLES

Lashing model	**Safety factor**			
	30°	**45°**	**70°**	**90°**
Model 1	1.47	1.04	0.78	0.74
Model 2	3.86	2.73	2.05	1.93
Model 3	2.32	1.64	1.24	1.16
Model 4	92.02	65.08	48.97	46.02
Model 5	82.75	58.52	44.04	41.38

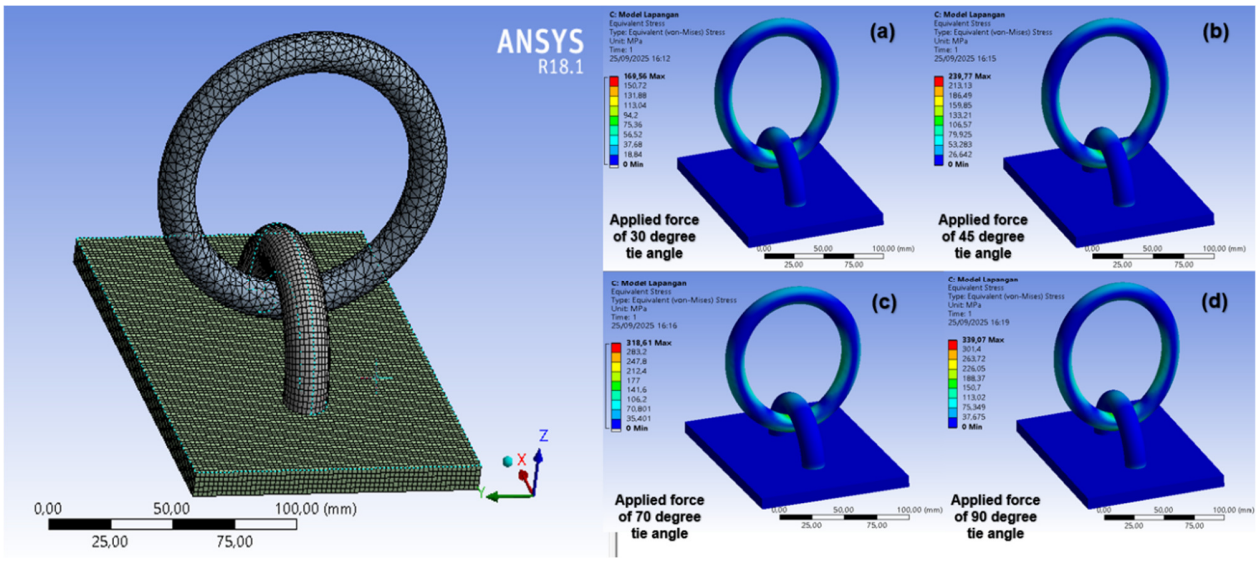

Fig. 7. FEM simulation results of Model 1 at different lashing angles: (a) 30°, (b) 45°, (c) 70°, and (d) 90°.

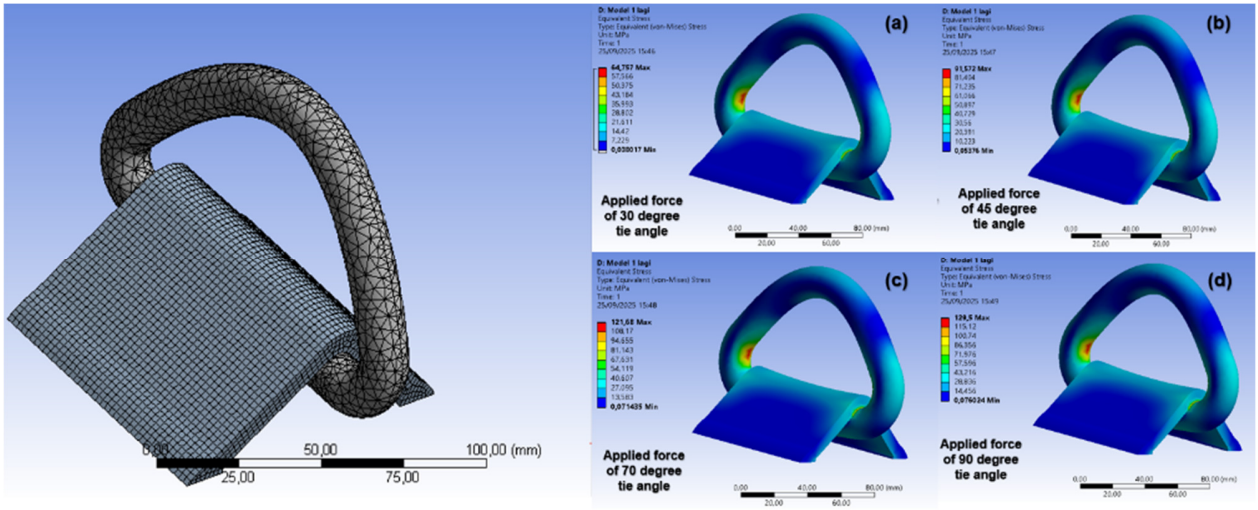

Fig. 8. FEM simulation results of Model 2 with D-ring at different lashing angles: (a) 30°, (b) 45°, (c) 70°, and (d) 90°.

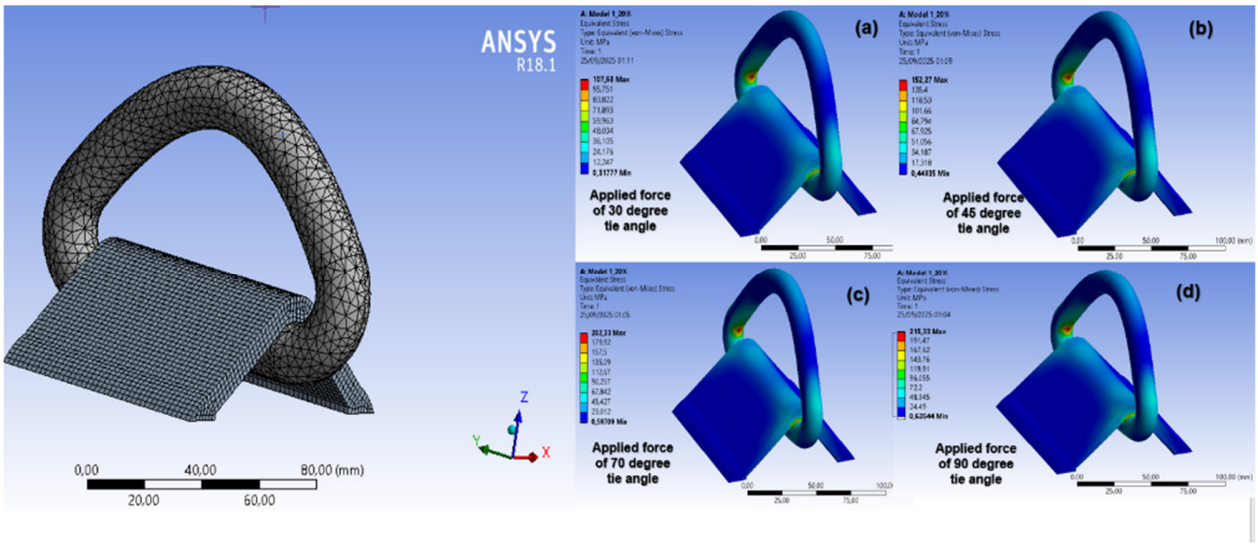

Fig. 9. FEM simulation results of Model 3 with D-ring having 20% diameter reduction at different lashing angles: (a) 30°, (b) 45°, (c) 70°, and (d) 90°.

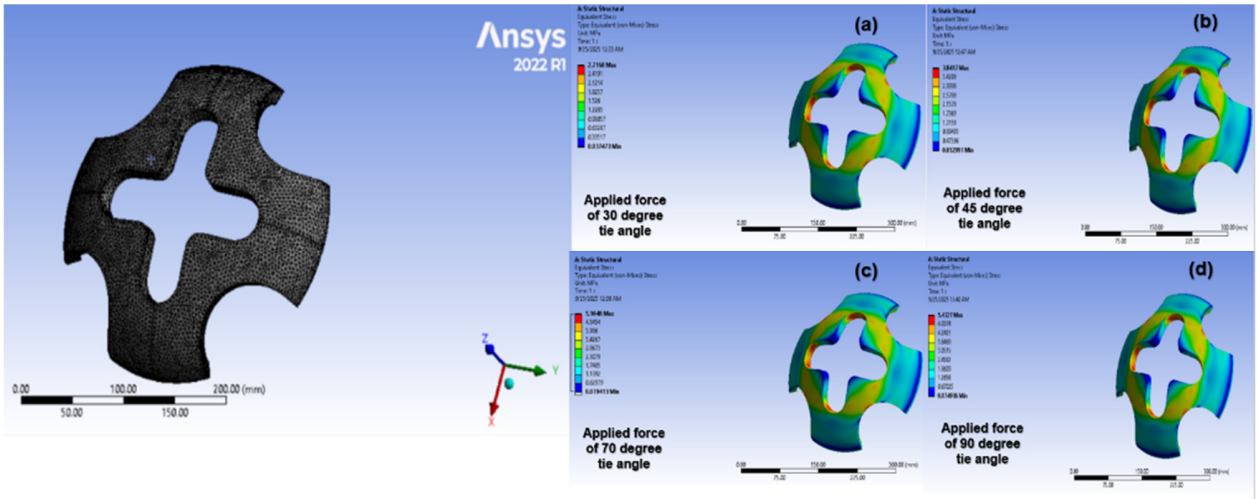

Fig. 10. FEM simulation results of Model 4 with convex at different lashing angles: (a) 30°, (b) 45°, (c) 70°, and (d) 90°.

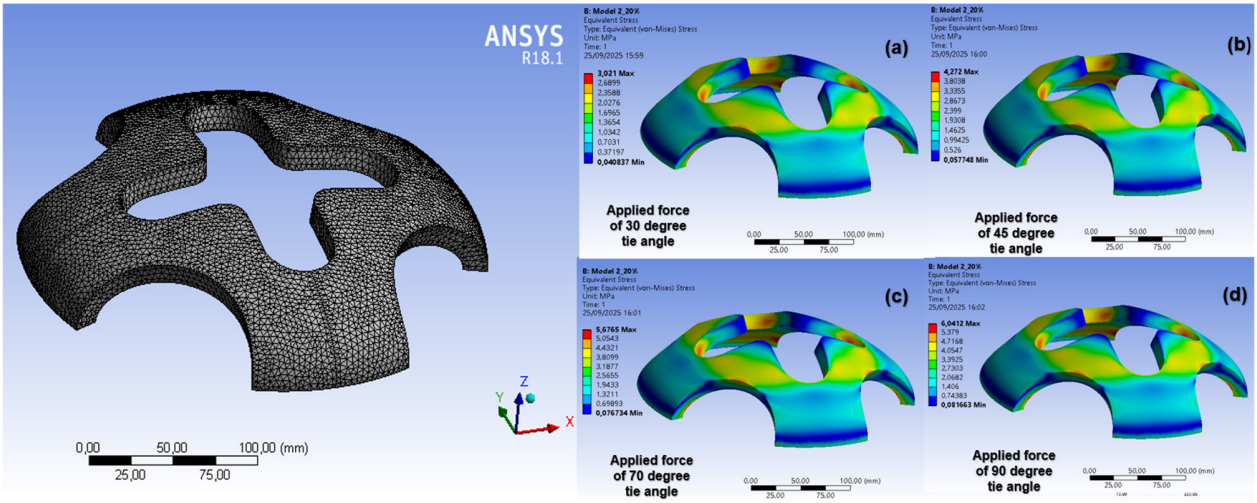

Fig. 11. FEM simulation results of Model 5 with convex having reduction of external radius at different lashing systems: (a) angle of 30°, (b) angle of 45°, (c) angle of 70°, and (d) angle of 90°.

IV. CONCLUSION

This research focuses on the lashing system on short crossing Roll-On-/Roll-Off (Ro-Ro) ferry routes, with the Balikpapan-Penajam Paser Utara route used as a case study. Lashing system modeling was carried out employing the Finite Element Method (FEM) numerical simulation. The aim was to determine the safety factor of the vehicle lashing system corresponding to the engagement angle, as specified in Indonesian government regulations. The results show that for all lashing system models, the von Mises stress increases linearly with the increase in engagement angle. Furthermore, the safety factor of the lashing system decreases with increasing vehicle lashing angle. Model 1, in particular, was revealed to be unsafe at 70° and 90°. In contrast, other models were safe at all lashing angles. Based on the findings of this study, it can be concluded that a higher lashing angle increases the available space on the deck of a Ro-Ro ferry. These findings provide guidelines for the regulators to increase lashing angles, which are limited to 60°. A higher lashing angle will create more space on the deck of the Ro-Ro ferries, possibly increasing the income of the ferry operators.

ACKNOWLEDGMENT

This research was funded by research grants provided by the Ministry of Higher Education, Science, and Technology of Indonesia, with contract numbers: 0070/C3/AL.04/2025 and 17614/IT10.L1/ PPM.04/2025.

REFERENCES

[1] S. Sadya, "Ada 19 Kecelakaan Pelayaran di Indonesia pada 2021," *Automotive and Transportation*, Sep. 2022. https://dataindonesia.id/otomotif-transportasi/detail/ada-19-kecelakaan-pelayaran-di-indonesia-pada-2021.

[2] R. Mustajab, "Terdapat 13 Kecelakaan Pelayaran Di Indonesia Pada 2022," *Automotive and Transportation*, Jan. 2023. https://dataindonesia.id/otomotif-transportasi/detail/terdapat-13-kecelakaan-pelayaran-di-indonesia-pada-2022.

[3] *Buku Statistik Investigasi Kecelakaan Transportasi Semester I Tahun 2022*. Jakarta, Indonesia: Komite Nasional Keselamatan Transportasi, 2022.

[4] H. Hasanudin, A. D. Saputra, A. N. Yulianto, and S. Sujantoko, "A Comparative Analysis of the Stability of Open-Deck River Boats Using Righting Moment and GM0 Based Criteria," *Kapal: Jurnal Ilmu Pengetahuan dan Teknologi Kelautan*, vol. 22, no. 2, pp. 151–161, Jul. 2025, https://doi.org/10.14710/kapal.v22i2.70447.

[5] *International Code on Intact Stability, 2008*. London, UK: International Maritime Organization, 2008.

[6] *Regulation of the Minister of Transportation Number PM 115 of 2016 Concerning Procedures for Transporting Vehicles on Ships*. Jakarta, Indonesia: Ministry of Transportation Indonesia, 2016.

[7] *Peraturan Menteri Perhubungan Nomor PM 30 Tahun 2016 tentang Kewajiban Pengikatan Kendaraan Pada Kapal Angkutan Penyeberangan*. Jakarta, Indonesia: Ministry of Transportation Indonesia, 2016.

[8] *Peraturan Menteri Perhubungan Republik Indonesia Nomor PM 26 Tahun 2019 Tentang Standar Pelayanan Minimal Angkutan Penyeberangan*. Jakarta, Indonesia: Ministry of Transportation Indonesia, 2019.

[9] P. Crossland and K. Rich, "A Method for Deriving MII Criteria," in *Conference on Human Factors in Ship Design and Operation*, London, UK, Sep. 2000.

[10] L. Zheng *et al.*, "Large-Signal Stability Analysis of All-Electric Ships with Integrated Energy Storage Systems," *IEEE Transactions on Industry Applications*, vol. 61, no. 5, pp. 7736–7749, Sep. 2025, https://doi.org/10.1109/TIA.2025.3550139.

[11] M. Gucma and P. Jabłoński, "Review of Dynamic Risk Assessment Methods for Navigation Safety of Ro-Pax Vessels," *ce/papers*, vol. 8, no. 3–4, pp. 395–401, Sep. 2025, https://doi.org/10.1002/cepa.3348.

[12] H. S. Kim *et al.*, "Design and Structural Safety Assessment of a Hinge-Based Hoistable Car Deck for Ro-Ro Vessels," *Journal of Marine Science and Engineering*, vol. 13, no. 9, p. 1662, Aug. 2025, https://doi.org/10.3390/jmse13091662.

[13] T. Kuroda, "Study of Parameters for Excessive Acceleration Failure Mode in Design Stage," *Ocean Engineering*, vol. 350, p. 124250, Mar. 2026, https://doi.org/10.1016/j.oceaneng.2026.124250.

[14] U. Khalid, "Investigation of Ship Vulnerability to Second Generation Intact Stability Criteria (SGISC) Based Failure Modes in Different Sea Areas," Master's Thesis, Norwegian University of Science and Technology, Trondheim, Norway, 2025.

[15] M. Konidaris, "Excessive Acceleration Second Generation Intact Stability Criteria Compared with Cargo Securing Manual," Diploma Thesis, National Technical University of Athens, Athens, Greece, 2024.

[16] H. Yang, Z. Jin, K. Chen, and Y. Li, "Extrema Estimation of Vehicle-bridge Interaction Responses Under Crosswind via Probabilistic Decoupling," *Journal of Wind Engineering and Industrial Aerodynamics*, vol. 270, p. 106353, Mar. 2026, https://doi.org/10.1016/j.jweia.2026.106353.

[17] S. Wang, J. Ren, X. Jiao, Z. Liu, and C. G. Soares, "A Time-domain Framework for Ship Motions Analysis Incorporating a Quadtree-Based Non-Linear Force Model," *Ocean Engineering*, vol. 343, p. 123430, Jan. 2026, https://doi.org/10.1016/j.oceaneng.2025.123430.

[18] D. Chrismianto, H. Yudo, B. A. Adietya, A. Firdhaus, and A. Abel Salassella, "Numerical Analysis of the Effect of Passive Free Surface Tank on Rolling Motion of Batang-Type Traditional Fishing Vessel," *TransNav, the International Journal on Marine Navigation and Safety of Sea Transportation*, vol. 19, no. 2, pp. 407–416, 2025, https://doi.org/10.12716/1001.19.02.09.

[19] A. M. Ibrahim and C. Q. Judge, "Investigations of Hull Girder Slamming Factor for a Semi-Displacement Vessel Using Model Testing," *Applied Ocean Research*, vol. 150, p. 104084, Sep. 2024, https://doi.org/10.1016/j.apor.2024.104084.

[20] I. K. A. P. Utama *et al.*, "Seakeeping Performance of Warship Catamaran under Varied Hull Separation and Wave Heading Conditions: An Integrated Numerical and Experimental Studies," *Pomorstvo*, vol. 38, no. 2, pp. 275–296, Dec. 2024, https://doi.org/10.31217/p.38.2.9.

[21] A. I. Wulandari, A. Sulisetyono, and I. K. A. P. Utama, "The Influence of Hull and Tunnel Geometry on Resistance and Seakeeping Behavior of Flat Side-inside Catamaran," *Ships and Offshore Structures*, pp. 1–35, Jul. 2025, https://doi.org/10.1080/17445302.2025.2529968.

[22] N. M. G. Zakaria, "Effect of Ship Size, Forward Speed and Wave Direction on Relative Wave Height of Container Ships in Rough Seas," *Journal of the Institution of Engineers*, vol. 73, no. 3, pp. 21–34, Sep. 2009.

[23] P.-H. Liu *et al.*, "Stress Influence Matrix on Hot Spot Stress Analysis for Welded Tubular Joint in Offshore Jacket Structure," *Ocean Engineering*, vol. 251, p. 111103, May 2022, https://doi.org/10.1016/j.oceaneng.2022.111103.

[24] E. V. Arcieri, S. Baragetti, and Ž. Božić, "Stress Assessment and Fracture Surface Analysis in a Foreign Object Damaged 7075-T6 Specimen Under Rotating Bending," *Engineering Failure Analysis*, vol. 138, p. 106380, Aug. 2022, https://doi.org/10.1016/j.engfailanal.2022.106380.

[25] Y.-Z. Wang, G.-Q. Li, Y.-B. Wang, and Y.-F. Lyu, "Simplified Method to Identify Full Von Mises Stress-Strain Curve of Structural Metals," *Journal of Constructional Steel Research*, vol. 181, p. 106624, Jun. 2021, https://doi.org/10.1016/j.jcsr.2021.106624.

[26] A. Silva-Campillo, L. Ulla-Campos, J. C. Suárez-Bermejo, and M. A. Herreros-Sierra, "Effect of Bow Hull Form on the Buckling Strength Assessment of the Corner Bracket Connection," *Ocean Engineering*, vol. 265, p. 112562, Dec. 2022, https://doi.org/10.1016/j.oceaneng.2022.112562.

[27] A. Popa, M.-G. Manea, and M.-V. Ristea-Komornicki, "FEM Structural Analysis for Ship's Beam Modification: A Case Study," *Engineering, Technology & Applied Science Research*, vol. 14, no. 4, pp. 15848–15853, Aug. 2024, https://doi.org/10.48084/etasr.7885.

[28] *Rules for the Classification and Construction. Part 1 Seagoing Ship. Volume V Rules for Materials*, vol. V. Jakarta, Indonesia: Biro Klasifikasi Indonesia, 2025.

[29] H. Cui, Z. Chen, R. Hu, and Q. Ding, "Ultimate Strength Assessment of Hull Girders Considering Elastic Shakedown Based on Smith's Method," *Ocean Engineering*, vol. 293, p. 116695, Feb. 2024, https://doi.org/10.1016/j.oceaneng.2024.116695.

[30] J. Abedin, "Structural Optimisation of Ship Hull Using Finite Element Method," PhD thesis, Newcastle University, Newcastle, UK, 2025.

[31] A. Pintilie, M.-G. Manea, O. Cristea, P. Burlacu, D. Mărăżescu, and C.-P. Clinci, "FEM Structural Analysis and CAD Hull Modelling for a Bulk Carrier - a Case Study," *TransNav, the International Journal on Marine Navigation and Safety of Sea Transportation*, vol. 19, no. 2, pp. 503–514, 2025, https://doi.org/10.12716/1001.19.02.20.

[32] B. Liu and C. Guedes Soares, "Ultimate Strength Assessment of Ship Hull Structures Subjected to Cyclic Bending Moments," *Ocean Engineering*, vol. 215, p. 107685, Nov. 2020, https://doi.org/10.1016/j.oceaneng.2020.107685.

[33] G. Jagite and F. Bigot, "Numerical Investigation of the Hull Girder Ultimate Strength Under Realistic Cyclic Loading Derived from Long-term Hydroelastic Analysis," *Ships and Offshore Structures*, vol. 18, no. 4, pp. 515–528, Apr. 2023, https://doi.org/10.1080/17445302.2022.2035566.

[34] J. M. Pérez-Canosa and J. A. Orosa, "A New Methodology for Optimization of Lashing Lines in the Securing Arrangement of Non-Standardized Cargo on Ships," *Applied Sciences*, vol. 14, no. 23, p. 11442, Dec. 2024, https://doi.org/10.3390/app142311442.

[35] M. Li, G. Wang, K. Liu, Y. Lu, and J. Wang, "Experimental and Numerical Analysis of Supporting Forces and Lashing Forces in a Ship Cargo Securing Scheme," *Journal of Marine Science and Engineering*, vol. 12, no. 1, p. 158, Jan. 2024, https://doi.org/10.3390/jmse12010158.

[36] *Ansys Academic Research*. Ansys, Inc, Canonsburg, PA, USA, 2021, [Online]. Available: https://www.ansys.com/en-in/academic.

[37] F. Fernandes, N. Sousa, F. S. Silva, Ó. Carvalho, and S. O. Catarino, "A Contemporary Systematic Review on Deterministic Numerical Simulations of Light Propagation in Head Tissues," *Biophysical Reviews*, Jan. 2026, https://doi.org/10.1007/s12551-025-01403-w.

[38] H. Cui, R. Hu, Z. Chen, and L. Huang, "Analysis of Ultimate Strength of Bulk Carrier Considering Elastic Shakedown Under Cyclic Bending Moment," *Chinese Journal of Ship Research*, vol. 20, no. 3, pp. 174–183, Jun. 2025.